

## MODELING OF STATIC LIQUEFACTION AND EVOLVING FAILURE MODES

Nathalie Boukpeti\*, Andrew Drescher \*\*

\*University of Liege, Chemin des Chevreuils 1, B-4000 Liege 1, Belgium

\*\*University of Minnesota, 500 Pillsbury Dr SE, Minneapolis, MN55455, U.S.A.,

**Summary** Considered are the elasto-plastic and elasto-viscoplastic versions of the Superior sand model for describing static liquefaction of granular deposits. Limit points and instability in stress-controlled undrained loading are analyzed. Examples of the effect of loading rate on shear band formation and growth of accelerated deformation in an inertial process in biaxial compression numerical simulations also are given.

### Refined Superior sand model

Loosely-packed, water-saturated granular deposits (sands, mine tailings) are prone to spontaneous loss of strength and accelerated deformation process when subject to increasing stress-controlled loading (static liquefaction). Due to increase in pore-water pressure the ensuing process transforms a solid-like material into a liquid-like medium. The process may grow unlimitedly, or terminate when the pore-water pressure drops and the material regains its strength. This behavior is described by the elasto-plastic refined Superior sand model formulated within the framework of critical state concept in [3], and subsequently analyzed and generalized in [1, 2, 5]. The elastic deformations are governed by a pressure-dependent elasticity. The evolution of plastic deformations is defined by a closed and smooth yield surface with configuration hardening parameter, and a non-associated flow rule. In terms of triaxial compression invariants  $p'$ ,  $q$ ,  $\varepsilon_p$ , and  $\varepsilon_q$ , the yield condition, plastic potential, and hardening rule are given by

$$F = q^2 - L^2 p'^2 \left[ \frac{1+s}{s} \left( 1 - \frac{p'}{p'_F} \right) \right]^{2s} = 0, \quad G = q^2 - M^2 p'^2 \left[ \left( \frac{p'_G}{p'} \right)^{\frac{1}{2r}} - 1 \right]^{2r} = 0 \quad (1)$$

$$\dot{p}'_F = p'_F \frac{v}{\lambda - \kappa} \dot{\varepsilon}_p + p'_F \sqrt{(\alpha \dot{\varepsilon}_q^{vp})^2 + (\dot{\varepsilon}_p^{vp})^2} \left\langle m \left( \frac{p'_F}{p'_F^*} - 1 \right) \right\rangle \quad (2)$$

where  $v$  is the specific volume,  $L$ ,  $M$ ,  $m$ ,  $r$ ,  $s$ ,  $\alpha$ ,  $\kappa$ , and  $\lambda$  are constants, and  $p'_F^*$  is a parameter of the reference surface. Examples of the stress-strain curves and stress paths obtained in undrained loading are depicted in Fig. 1.

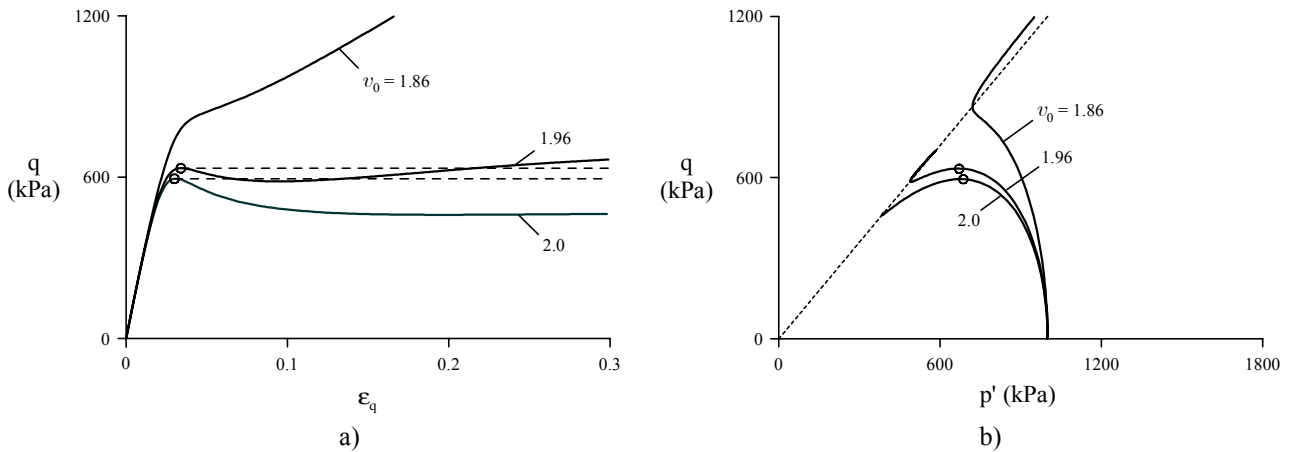


Fig.1 Elasto-plastic response and instability points; a) strain- and stress-control, b) stress paths

The response of the model can be characterized by its limiting and instability points. These depend on the process control variable – stress or strain. In stress-controlled loading, the instability occurs at the first limit point where

$$W_2 = \dot{q} \dot{\varepsilon}_q = 0 \quad (3)$$

as indicated in Fig. 1 by circles. The severity (energy) of liquefaction can be assessed from the excess of applied load over the reduced strength, and in ideal conditions amounts to the area between the applied stress and material stress-strain curve.

To account for the observed experimentally delayed liquefaction under constant load (creep), and the dependence of the stress-strain curves on the rate of strain-controlled loading [4], the refined Superior sand model was modified within the framework of viscoplasticity of Perzyna (1963). The resulting stress-strain curves in strain-controlled loading  $\dot{\epsilon}_q = \dot{\epsilon}_{q0}$ , and in stress-controlled loading  $\dot{q} = \dot{q}_0$ , are governed, respectively, by

$$\frac{\dot{q}}{\dot{\epsilon}_q} = 3\mu - \frac{\frac{6q\mu}{\tau\dot{\epsilon}_{q0}} \left\langle \frac{p'_d}{p'_F} - 1 \right\rangle^n}{\sqrt{\left\{ p'\eta^2 \left[ \left( \frac{M}{\eta} \right)^{1/r} - 1 \right]^2 + 4q^2 \right\}}}, \quad \frac{\dot{q}}{\dot{\epsilon}_q} = \frac{\tau\dot{q}_0 \sqrt{\left\{ p'\eta^2 \left[ \left( \frac{M}{\eta} \right)^{1/r} - 1 \right]^2 + 4q^2 \right\}}}{\frac{\tau q_0}{3\mu} \sqrt{\left\{ p'\eta^2 \left[ \left( \frac{M}{\eta} \right)^{1/r} - 1 \right]^2 + 4q^2 + 2q \left\langle \frac{p'_d}{p'_F} - 1 \right\rangle^n}} \quad (4)$$

where  $\tau$  is the coefficient of viscosity,  $\eta = q/p'$ ,  $\mu$  and  $n$  are constants, and  $p'_d$  is a parameter of the dynamic yield surface. The rate-dependence of the model affects the limiting states at which an accelerated process (instability) may commence. In fact, condition (3) no longer applies, because, in contrast to strain-controlled loading, in stress-controlled loading no apparent softening occurs. The onset of accelerated process takes place when

$$W_3 = q\ddot{\epsilon}_q = 0 \quad (5)$$

and this is demonstrated in Fig. 2

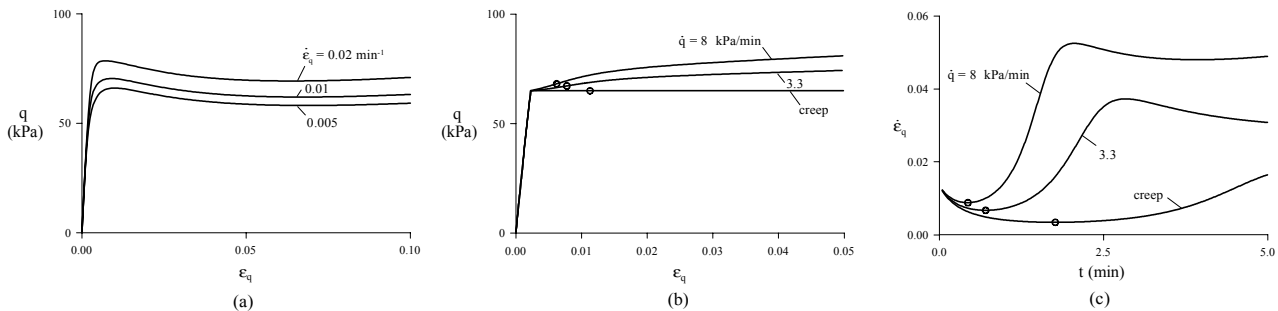


Fig. 2 Elasto-viscoplastic response and instability points; a) strain-control, b) stress-control, c) evolution of strain-rate

### Numerical simulations

To illustrate the model predictions further, two types of numerical simulations (FLAC) of the undrained, plane-strain, biaxial compression test were performed. In the first, the elasto-plastic model was used to demonstrate the effect of hydro-mechanical coupling on the formation of shear bands in a specimen subjected to strain-controlled loading. The results confirm the theoretical findings in [7] that low hydraulic conductivity and high loading rates support the occurrence of shear bands in the case of contractant material; in essence, the process is controlled by a characteristic dimensionless parameter. In the second type of simulation, the specimen made of the elasto-viscoplastic material was subjected to load-controlled loading in a fully inertial system that allows for spontaneous growth of accelerated deformation of the specimen in the post-stable regime. Demonstrated is the resulting difference in stress measurements at the various locations in the specimen. The results of both simulations have direct implications in designing and conducting physical tests on water-saturated granular deposits, and in their data interpretation.

### References

- [1] Boukpeti, N., Drescher, A.: Triaxial behavior of refined Superior sand model. *Comp. Geotech* **26**: 65-81, 2000.
- [2] Boukpeti, N., Mróz, Z., Drescher, A.: A model for static liquefaction in triaxial compression and extension. *Canadian Geotech. J.* **39**: 1243-1253, 2002.
- [3] Drescher, A., Mróz, Z.: A refined Superior sand model. *Num. Models Geomech, NUMOG VI*, G. N. Pande and S. Pietruszczak. eds., A.A. Balkema, 21-26, 1997.
- [4] Lade, P.V., Yamamuro, J., Bopp, P.: Influence of time effects on instability of granular materials. *Comp. Geotechnics* **20**: 179-193, 1997.
- [5] Mróz, Z., Boukpeti, N., Drescher, A.: Constitutive model for static liquefaction. *Int. J. Geomech* **3**: 133-144, 2003.
- [6] Perzyna, P.: The constitutive equations for rate sensitive plastic materials. *Quart. Appl. Math* **20**: 321-332, 1963.
- [7] Vardoulakis, I.: Deformation of water-saturated sand: I. Uniform undrained deformation and shear banding, II. Effect of pore water flow and shear banding, *Géotechnique* **46**: 441-456, 1996.